The Planetary Science Journal, 3:132 (9pp), 2022 June https://doi.org/10.3847/PSJ/ac6dce

Moderately High Obliquity Promotes Biospheric Oxygenation

Megan N. Barnett[1] and Stephanie L. Olson[2]
[1] Department of the Geophysical Sciences, University of Chicago, Chicago, IL 60637, USA; meganbarnett@uchicago.edu
[2] Department of Earth, Atmospheric, and Planetary Sciences, Purdue University, West Lafayette, IN 47907, USA
Received 2022 February 8; revised 2022 April 27; accepted 2022 May 5; published 2022 June 6

Abstract

Planetary obliquity is a first-order control on planetary climate and seasonal contrast, which has a number of cascading consequences for life. How moderately high obliquity (obliquities greater than Earth's current obliquity up to 45°) affects a planet's surface physically has been studied previously, but we lack an understanding of how marine life will respond to these conditions. We couple the ROCKE-3D general circulation model to the cGENIE 3D biogeochemical model to simulate the ocean biosphere's response to various planetary obliquities, bioessential nutrient inventories, and biospheric structure. We find that the net rate of photosynthesis increased by 35% and sea-to-air flux of biogenic oxygen doubled between the 0° and 45° obliquity scenarios, which is an equivalent response to doubling bioessential nutrients. Our results suggest that moderately high obliquity planets have higher potential for biospheric oxygenation than their low-obliquity counterparts and that life on moderately high obliquity habitable planets may be easier to detect with next-generation telescopes. These moderately high obliquity habitable planets may also be more conducive to the evolution of complex life.

Unified Astronomy Thesaurus concepts: Astrobiology (74); Biosignatures (2018); Exoplanets (498); Habitable planets (695); Ocean-atmosphere interactions (1150)

1. Introduction

Habitable exoplanets will differ from Earth in several ways that may affect biogeochemical cycles, biospheric productivity, and biospheric detectability. One potential characteristic that might differ between Earth and exoplanets is planetary obliquity, or the angle between the planet's axis of rotation and orbital axis (Figure 1, left panel). Planetary obliquity can significantly affect planetary climate. Planets with larger obliquities have larger-amplitude seasonal variations (e.g., Williams and Kasting 1997; Spiegel et al. 2009; Armstrong et al. 2014; Nowajewski et al. 2018; Guendelman & Kaspi 2019) owing to differences in seasonal stellar energy distribution at the planetary surface with increasing obliquity. Moderately high obliquity planets also experience a more uniform distribution of stellar energy across the planetary surface on annual average, leading these planets to be warmer on average than their low-obliquity counterparts (e.g., Linsenmeier et al. 2015; Wang et al. 2016; Nowajewski et al. 2018; Guendelman & Kaspi 2019; Kang 2019a; Palubski et al. 2020; Komacek et al. 2021).

There are a wide range of obliquities among the terrestrial and giant planets in our solar system, ranging from slight to extreme. The terrestrial planets span a wide range of obliquities, with Mercury and Venus having obliquities very close to 0° (0.1° and 177.4°, respectively, with Venus orbiting retrograde) and Earth and Mars currently having moderate obliquities of 23.4° and 25°, respectively. Earth's obliquity is believed to have varied within the moderate range of 22.1° to 24.5° for at least the past 400 Myr (Williams 1993), while Mars's obliquity may have varied between 0.2° to ∼60° over the past 10–45 Myr (Bills 1990; Laskar & Robutel 1993; Laskar et al. 2004). Among the outer solar system giant planets, Jupiter, Saturn, and Neptune have obliquities of 3°, 26.7°, and 29.6°, while only Uranus has a much higher obliquity of 98°. These vastly different obliquities and their evolution in our own solar system suggest that exoplanet obliquities likely vary widely as well, though there are currently very few constraints on these measurements for individual exoplanets (Bryan et al. 2020).

Planetary obliquity does not just affect the planet's climate. Olson et al. (2020) used ROCKE-3D (Way et al. 2017), a state-of-the-art ocean-atmosphere general circulation model (GCM), to investigate the effect of planetary obliquity on ocean dynamics and marine habitats. They found that increasing planetary obliquity from 0° to 45° yielded warmer climates and increased seasonal variability of the mixed layer depth (the depth to which the water column is homogeneous owing to turbulence and mixing). Olson et al. (2020) argued that ocean circulation patterns changes due to increased planetary obliquity could yield greater nutrient recycling, greater biosphere productivity, and greater biosignature accumulation. However, the GCM used by Olson et al. (2020) lacked explicit representation of life. We address that gap here.

In this work, we couple winds from a GCM (ROCKE-3D) with a marine biogeochemical model (cGENIE) to explicitly simulate the response of an Earth-like biosphere to moderately high planetary obliquity (Section 2). Section 3 describes the biospheric response to various planetary obliquities, phosphate inventories, and biospheric structure. We then discuss our results and their implications for planetary oxygenation, biological evolution, and exoplanet life detection in Section 4. These findings are summarized in Section 5.

2. Methods

We investigate the response of ocean life to planetary obliquity using the ROCKE-3D GCM leveraged by Olson et al. (2020) to force cGENIE, a 3D biogeochemical model originally developed by Ridgwell et al. (2007). cGENIE couples

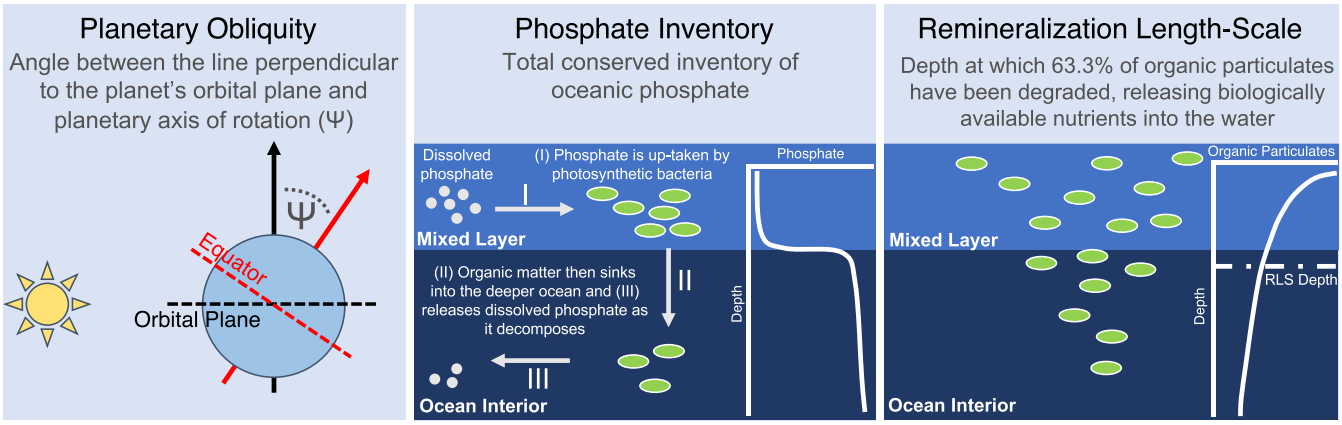

Figure 1. Depiction and definitions of parameters of interest varied in models in this paper. The white dashed–dotted horizontal line in the right panel indicates the depth of the RLS in the schematic.

a 3D marine biogeochemistry model to a 3D ocean circulation model with dynamic-thermodynamic sea ice, all under an energy–moisture balance model with bulk atmospheric chemistry. While cGENIE has historically been used to simulate the geologically recent past and near future, it has since been extended to include a full treatment of methane-based atmospheric chemistry, ocean/atmosphere methane cycling, and methane-based metabolisms to enable the simulation of low oxygen biospheres (Olson et al. 2013, 2016; Reinhard et al. 2020).

Our experiments use the same topography and bathymetry as the original ROCKE-3D experiments from Olson et al. (2020), and we prescribe steady-state surface wind output from their experiments to drive ocean circulation within cGENIE. Prescribing steady-state winds greatly reduces the computational cost of our simulations, allowing us to explore a larger swath of parameter space in our simulations. Using steady-state, rather than time-variable, winds is acceptable because wind-driven upwelling was only weakly sensitive to obliquity in the simulations from Olson et al. (2020). In contrast, the wind-mixed layer depth varied dramatically between seasons in moderately high obliquity scenarios owing to differences in thermal stratification. It is this mixed layer seasonality that Olson et al. (2020) argued will have the greatest affect on biogeochemical cycles on moderately high obliquity worlds, and we include this effect in our simulations.

We prescribe an atmosphere with fixed 1% present atmospheric levels of oxygen, similar to Proterozoic Earth (e.g., Lyons et al. 2014). Prescribing atmospheric oxygen at low levels allows us to explore oxygen dynamics on planets that have have not yet experienced a large-scale oxygenation despite the presence of oxygenic photosynthesis, like early Earth, where biological oxygen production preceded atmospheric oxygenation by several hundred million years (e.g., Planavsky et al. 2014).

Unless otherwise specified, all other model parameters are set at their preindustrial Earth values (e.g., solar insolation is set at 1368 W m^{-2}, and pCO_2 is set at 278 ppmv). This includes eccentricity, which is equal to 0.0167, with perihelion occurring during the northern hemisphere winter and introducing slight seasonality even in our 0° obliquity scenario.

We consider four different planetary obliquity values, with two low planetary obliquities less than Earth's current obliquity (0° and 15°) and two moderately high planetary obliquities greater than Earth's current obliquity (30° and 45°). We choose these obliquity values to sample the same obliquity space as Olson et al. (2020), whose experiments provided necessary wind field inputs for our experiments.

In addition to planetary obliquity, we also test the effect of varying two key biosphere parameters. The first of these parameters is the total ocean phosphate inventory. Phosphate (PO_4^{3-}) is the carrier molecule for phosphorus, an essential element that limits biological activity on Earth over geologic timescales (Tyrrell 1999; Reinhard et al. 2017). As phosphate is a critical nutrient for life, it is important to understand how a range of phosphate inventories would affect life on potential habitable exoplanets.

The second parameter varied in our simulations is the remineralization length scale (RLS). Organic carbon decays according to the RLS within the cGENIE model, implemented as an *e*-folding depth at which 63.3% of particulate organic carbon (POC) and associated nutrients have been recycled. We vary this length scale to characterize how the depth distribution of POC remineralization affects nutrient cycles.

We run simulations where these three variables (phosphate inventory, RLS, and obliquity) are both varied independently and covaried, for a total of 80 distinct model configurations. Unless otherwise stated, all other model parameters are set to their present-day Earth values. We run the simulations until steady state is achieved (10,000 yr). Then, we calculate both annual and seasonal averages for each model output parameter from the final year of model evolution.

3. Results

3.1. Planetary Obliquity Scenarios

We first consider the results from a range of obliquity scenarios (0°–45°) with present-day Earth ocean phosphate inventory and RLS to determine planetary obliquity's effect on export POC, the flux of organic carbon produced by photosynthesis that evades remineralization in surface waters and sinks to the deeper ocean—leaving behind oxygen. We additionally quantify the response of sea-to-air oxygen flux resulting from photosynthesis. In these obliquity scenarios (ranging from 0° to 45°), annual total global export POC generally increases with increasing obliquity, with export POC increasing by 35% between the 0° and 45° obliquity scenarios. However, export POC reaches a minimum at 15° obliquity

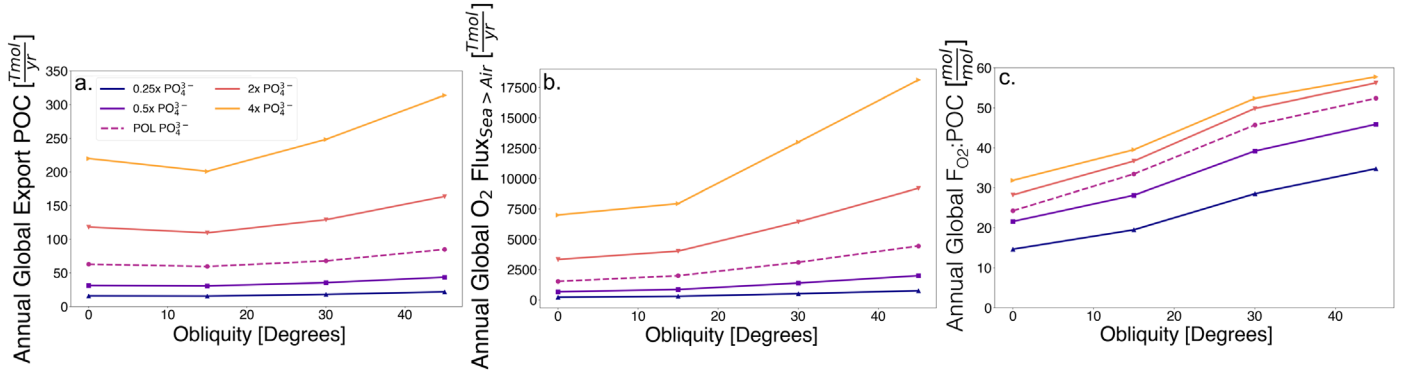

Figure 2. Export particulate organic carbon (POC; panel (a)), oxygen flux (F_{O_2}; panel (b)), and oxygen flux per unit organic carbon (F_{O_2}:POC; panel (c)) from varying phosphate levels at different obliquity levels. The POL label stands for present-day ocean levels and indicates the present-day Earth phosphate inventory scenario. Other scenarios are labeled with their modification factor times present-day ocean levels. RLS is tuned to match chemical profiles from Earth's present-day ocean and present-day obliquity (Ridgwell et al. 2007).

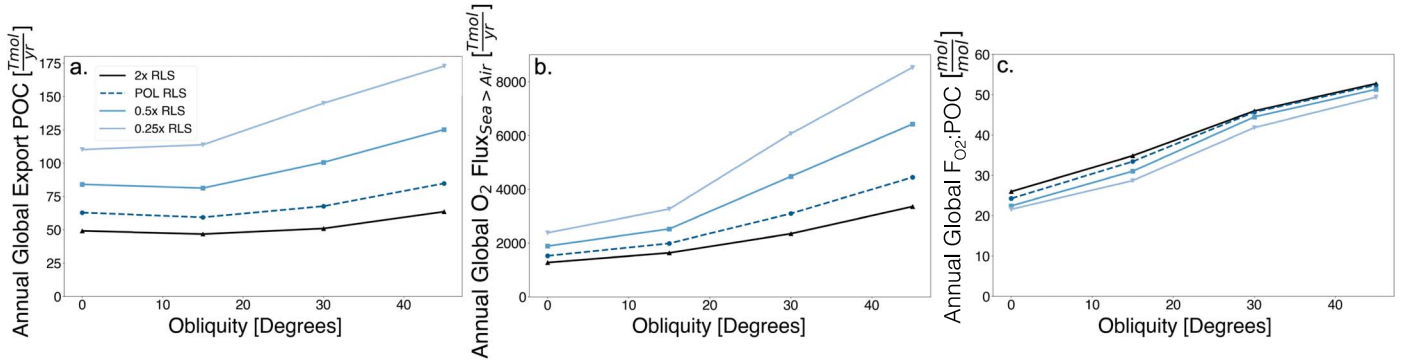

Figure 3. Export particulate organic carbon (POC; panel (a)), oxygen flux (F_{O_2}; panel (b)), and oxygen flux per unit organic carbon (F_{O_2}:POC; panel (c)) for scenarios with various RLSs (each scenario is labeled by the modifying factor times RLS) at different obliquity levels. Phosphate inventory in each of these experiments is set to POL.

(Figure 2(a), magenta line), decreasing by 5% between the 0° and 15° obliquity scenarios.

We also see that global oxygen sea-to-air flux (F_{O_2}) increases with obliquity. There is a twofold increase in F_{O_2} between the 0° obliquity and 45° obliquity scenarios (Figure 2(b), magenta line). While a portion of this increase in F_{O_2} from the ocean to the atmosphere is a consequence of increased photosynthesis, as evidenced by the increase in export POC values with increasing obliquity, the ratio of F_{O_2} to POC also increases with higher obliquity (Figure 2(c), magenta line). This increase in F_{O_2}:POC in moderately high obliquity scenarios suggests that physical effects caused by moderately high obliquity also contribute to the increase in F_{O_2} with higher obliquity.

3.2. Biospheric Sensitivity to Phosphate

We then simulate oceans with a range of phosphate inventories and planetary obliquity values. Increasing phosphate inventory in our simulations has an ∼1:1 effect on increasing export POC (Figure 2(a)). The phosphate inventory also affects the biospheric response to obliquity. The biosphere is relatively insensitive to obliquity when phosphate is scarce (0.25–0.5× POL), but export POC becomes increasingly sensitive to obliquity under phosphate replete conditions (2–4× POL).

This same trend is seen in F_{O_2} values as well (Figure 2(b)). At low phosphate inventory levels, F_{O_2} is relatively unaffected by obliquity. However, F_{O_2} increases more strongly with obliquity when phosphate is more abundant. At high phosphate inventory (2–4× POL), increasing obliquity from 0° to 45° yields greater that 2× F_{O_2}, an effect similar to doubling the phosphate inventory.

The ratio of F_{O_2} from sea to air to unit export POC experiences a similar twofold increase with obliquity increase from 0° to 45° to that caused by a doubling of phosphate inventory (Figure 2(c)). Unlike for F_{O_2} values, scenarios at every phosphate inventory value experienced a doubling in F_{O_2}:POC ratio with an obliquity increase from 0° to 45°.

3.3. Biospheric Sensitivity to Remineralization Length Scale

As POC sinks through the water column, nutrients are made available again for metabolic reactions such as photosynthesis through remineralization at depth and transport back to the photic zone. Remineralization is the first step in this process and occurs throughout the water column. The RLS affects the vertical distribution of nutrients in the water column and the timescale for their return to the surface. When RLSs are longer, nutrient-containing particles are able to settle deeper into the water column on average before they are processed and made available for transport back to the surface, leading to greater accumulation of nutrients at depth.

Simulations with shallower RLSs displayed increased POC export and biosphere activity (Figure 3(a)). The increase in POC export with shallower remineralization occurs because nutrients do not settle as far into the deep ocean and nutrients are more readily returned to the surface via wind-driven upwelling.

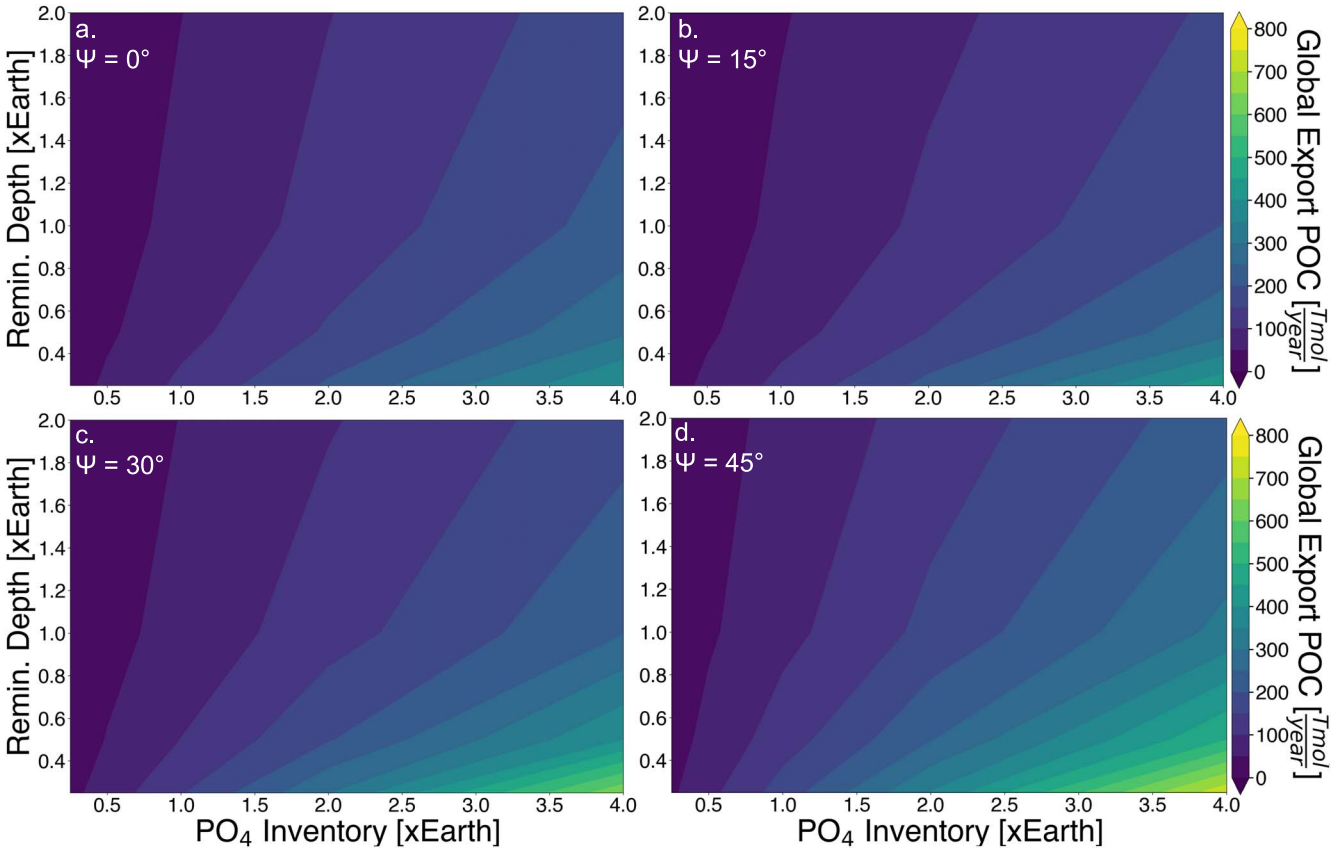

Figure 4. Global annual export particulate organic carbon for simulations with covaried phosphate inventory, RLS, and obliquity. We consider obliquities of 0° (panel (a)), 15° (panel (b)), 30° (panel (c)), and 45° (panel (d)). Annual global export POC increases with increasing phosphate inventory (Figure 2), decreasing RLS (Figure 3), and increasing obliquity.

We find that export POC only slightly increases with obliquity for experiments with longer RLSs. However, export POC increases with higher obliquity for scenarios with shorter RLSs (0.25–0.5× present ocean levels, or POL, Figure 3(a)). F_{O_2} increases by ∼3–4× with increasing obliquity and decreasing RLS in all our sensitivity experiments at POL phosphate inventory (Figure 3(b)). Moderately high obliquity is a stronger driver of F_{O_2} increase than RLS decrease, as halving RLS causes an increase in F_{O_2} of approximately 50%, while increasing obliquity from 0° to 45° results in greater than double F_{O_2} (⩾100% increase).

The ratio of F_{O_2} to export POC increases with increasing obliquity (Figure 3(c)) for all simulated RLSs. This result also supports our assertion that physical changes caused by increasing obliquity are partially responsible for the observed increase in F_{O_2}.

Additionally, we find that while F_{O_2} and POC alone decrease with deeper RLSs, F_{O_2}:POC ratio increases with deeper RLSs. F_{O_2} and export POC decrease with increasing RLS, as when the RLS is deeper, nutrients sink to deeper levels in the water column and decrease the amount of nutrients available for the surface biosphere. A decrease in photosynthesis due to a reduction of nutrients then leads to a decrease in oxygen production, and by extension F_{O_2} decrease. However, when we look at the F_{O_2}:POC ratio, we see this ratio increase with deeper remineralization depths. Although both F_{O_2} and POC decrease with increasing RLS, F_{O_2}:POC increases because deeper remineralization results in less near-surface oxygen consumption.

3.4. Additional Experiments

We ran a series of experiments in which we covaried obliquity, RLS, and phosphate inventory to explore potential synergistic effects introduced through covariance of these variables. Such effects could have profound implications for the potential for oxygen buildup on Earth-sized exoplanets.

The general trends for export POC, F_{O_2}, and F_{O_2}:POC ratio in response to increasing obliquity, phosphate inventory, and RLS previously discussed in Sections 3.1, 3.2, and 3.3 continue to hold true in the covarying simulations (Figures 4–6). Both export POC and F_{O_2} increase most strongly in response to increasing phosphate inventory, with second-order increases driven by decreasing RLS and increasing obliquity. When we increase phosphate inventory and decrease RLS in tandem, a synergistic effect is present. We find that scenarios with increased phosphate inventory and decreased remineralization depth yield >2× export POC and F_{O_2} levels than the sum of two independent scenarios with increased phosphate inventory and decreased RLS.

4. Discussion

4.1. Increased Obliquity Drives Enhanced Biological Activity and Atmospheric Oxygenation

The general increase in export POC with higher obliquity is driven by increased nutrient availability. As discussed earlier, Olson et al. (2020) predicted that increased seasonal deepening of the mixed layer depth with increasing obliquity during each hemisphere's winter would lead to increased nutrient cycling.

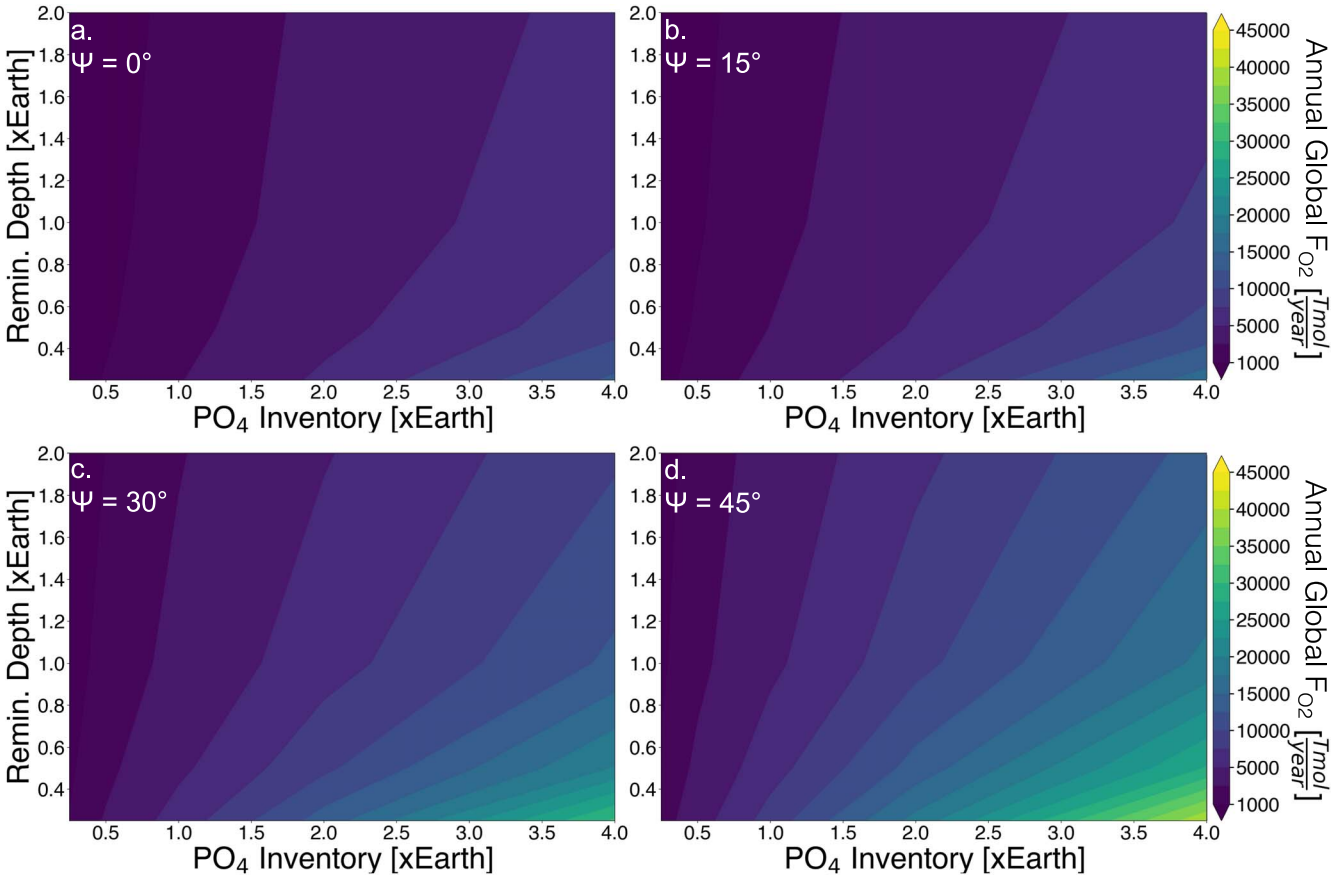

Figure 5. Annual global F_{O_2} for simulations with covaried phosphate inventory, RLS, and obliquity. We consider obliquities of 0° (panel (a)), 15° (panel (b)), 30° (panel (c)), and 45° (panel (d)). As seen in the single variable models, annual global F_{O_2} increases with increasing phosphate inventory, decreasing RLS, and increasing obliquity.

This increased seasonal deepening of the mixed layer depth occurs with increasing obliquity in our scenarios as well (Figure 7(a)).

Seasonal deepening of mixed layer depth in the winter hemisphere intensifies with increasing obliquity because as obliquity increases, the winter hemisphere receives less incident insolation. Reduced incident insolation leads to colder sea surface temperatures and weakened water density stratification, resulting in a deeper mixed layer depth. Deeper mixed layer depths allow for increased entrainment of nutrients from depth, resulting in higher surface phosphate concentrations (Figure 7(b)).

Varying seasonal nutrient availability significantly affects biological primary productivity throughout the year. In the 0° obliquity scenario, POC export rates do not significantly vary throughout the year owing to the lack of seasons (the slight variation between seasons displayed is due to the planet's nonzero eccentricity). However, for obliquity scenarios of 15° or higher, spring has the highest rate of POC export, followed by winter (Figure 7(c)). In the 45° obliquity scenario, spring export POC increases by approximately 2.5× in comparison to the 0° obliquity scenario, while winter export POC increases by a factor of two when compared to the 0° obliquity scenario. In the nonzero-degree obliquity scenarios, fall and summer have the lowest rates of POC export with summer POC export at slightly higher rates than in the fall.

POC export in the winter exceeds POC export in summer and fall owing to enhanced nutrient inventories in the surface ocean (Figure 7(c)). These nutrient rich waters are dredged up by the deepened mixed layer in these moderately high obliquity scenarios. However, although winter surface waters have an enhanced nutrient inventory, these nutrients cannot be entirely utilized owing to reduced insolation during the winter. This inhibits biological activity and therefore limits POC export until the spring. When winter ends, a "spring bloom" of heightened biological activity occurs when incident insolation begins to increase again after the dark winter season and provides residual nutrient-rich waters with light. Biological activity increases dramatically, fueled by both sufficient light and abundant nutrients, and leads to the observed maximum POC export in spring (Figure 7(c)). As a result of the deepened mixed layer and enhanced winter nutrient availability, the increases in seasonal export POC for moderately high obliquity scenarios lead to the observed increase in annual export POC with obliquity.

Though light and temperature do have significant effects on POC export in general, in our simulations these effects are negligible compared to the effect of nutrient availability. As obliquity increases, light is more evenly distributed over the planetary surface on annual average, but the total amount of light the planet's surface receives does not change, and so light cannot be the cause of the observed increase in annual export POC. Moderately high obliquity increases the amount of incident irradiation on a hemisphere during the summer months and decreases it during the winter months. One might then expect an increase in export POC during the summer and a

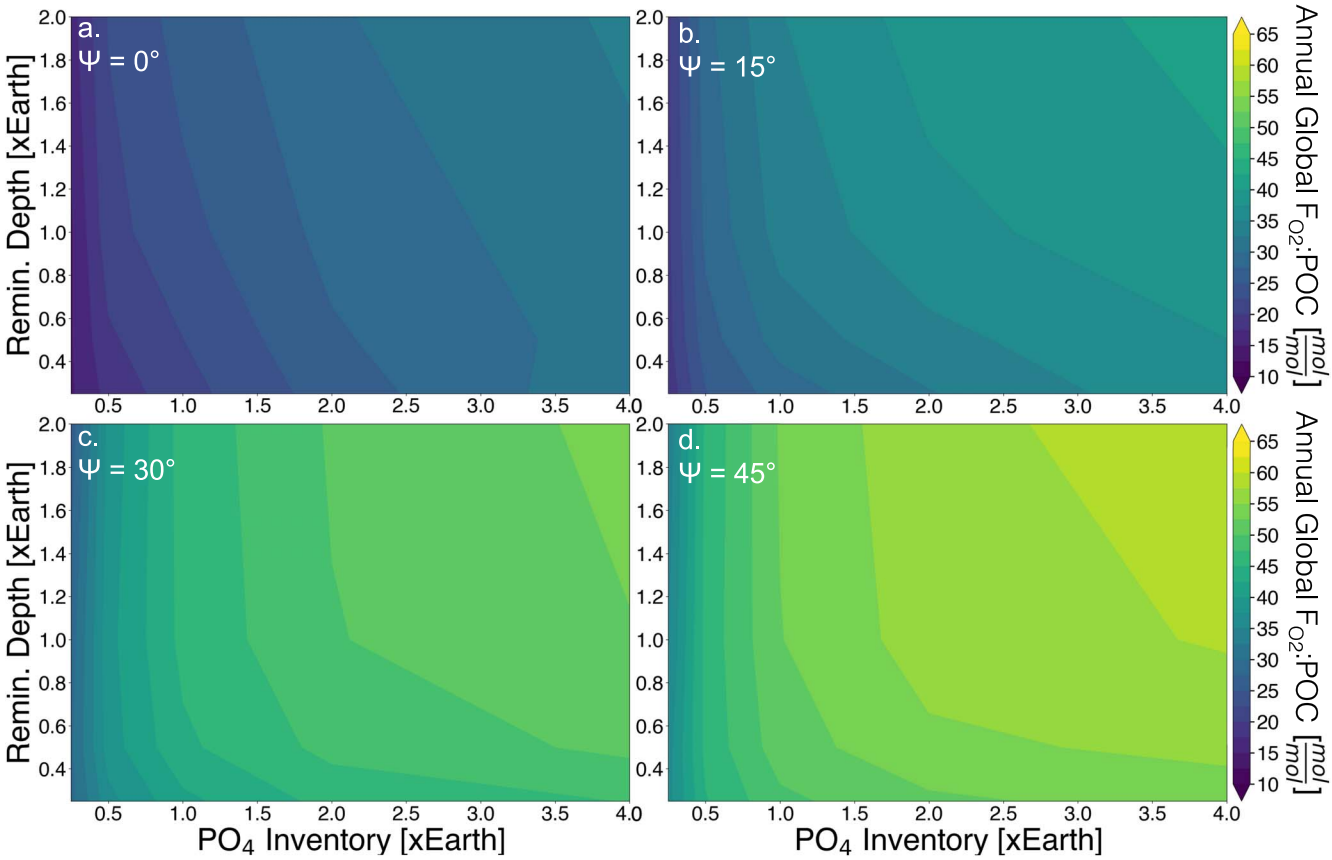

Figure 6. Annual global F_{O_2} per unit POC for simulations with covaried phosphate inventory, RLS, and obliquity. We consider obliquities of 0° (panel (a)), 15° (panel (b)), 30° (panel (c)), and 45° (panel (d)). Global average F_{O_2}:POC increases with increasing phosphate inventory, increasing RLS, and increasing obliquity.

decrease in the winter, which is not observed in our results owing to the overriding effect of nutrient availability. Additionally, in cGENIE's temperature-dependent export scheme, export POC increases with increasing temperature. One may then expect that larger temperature extremes due to increased seasonality would lead to increased export POC in the summer and decreased export POC in the winter. However, as we instead see that winter export POC surpasses summer export POC (Figure 7(c)), we conclude that nutrient availability is the dominant factor affecting export POC.

We find that both export POC and sea-to-air oxygen flux increase with increasing obliquity (Figures 2–5). This increase in F_{O_2} is a direct consequence of increased biological activity; as biological activity increases, there are more photosynthetic organisms performing photosynthesis, resulting in an increase in biogenic oxygen production. An interesting consequence of increased obliquity, however, is the effect of increasing obliquity on annual global oxygen flux per unit export POC. This increase implies that increased oxygen flux cannot be solely attributed to the increase in export POC.

If the increase in F_{O_2} with increasing obliquity was simply due to the increase in export POC with obliquity, the F_{O_2}:POC ratio would be constant across all considered planetary obliquity values, as produced oxygen would scale proportionally with increased primary productivity, which it is not (Figure 2). An increase in F_{O_2}:POC implies that physical effects are likely amplifying the increase in F_{O_2} with increasing obliquity.

The physical effects responsible for amplifying F_{O_2} increase with higher obliquity are decreased sea surface ice coverage and decreased solubility of oxygen in warmer water. Higher obliquity results in a more even distribution of insolation over the planetary surface. This leads to a decrease in the global average percentage of sea-ice coverage as obliquity increases (Figures 8(a), (c), (e), (g)) and warmer waters due to higher incident irradiation at the poles. As the sea-ice coverage decreases owing to the increase in obliquity and increase in ocean water temperature, a corresponding increase in oxygen flux from those now uncovered areas at high latitudes occurs (Figures 8(b), (d), (f), (h)). The resulting increase in oxygen flux occurs because (1) without ice coverage, these areas of open ocean are now able to exchange oxygen with the atmosphere with no physical barrier impeding gas exchange, and (2) oxygen is less soluble in warmer water (e.g., Wanninkhof 2014). Therefore, higher photosynthesis rates at the poles lead to enhanced sea-to-air fluxes of biogenic oxygen owing to the combined effects of increased surface area available for gas exchange and warmer ocean temperatures.

4.2. Moderately High Obliquity Increases Biosphere Detectability

Atmospheric oxygen may be a remotely detectable signature of life on other planets (e.g., Meadows et al. 2018). Although current telescopes are not designed to detect biotic levels of oxygen in exoplanet atmospheres (Lustig-Yaeger et al. 2019), next-generation telescopes such as the LUVOIR-like observatory recommended by the Astro2020 Decadal Survey would be able to detect biotic levels of oxygen in exoplanet atmospheres depending on cloud conditions and exposure times (Wang et al. 2018). As we

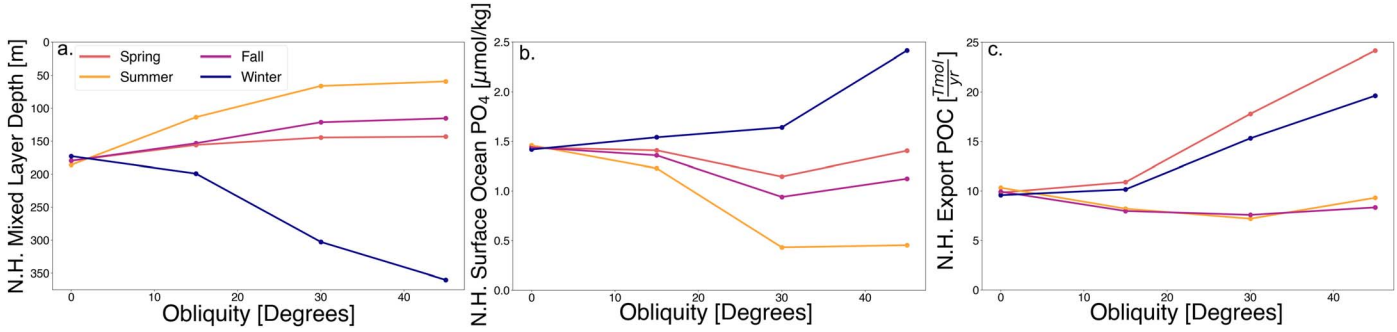

Figure 7. Seasonal Northern Hemisphere (N.H.) values for average mixed layer depth (panel (a)), total surface ocean PO_4 (panel (b)), and total export POC (panel (c)).

have shown in our experiments, moderately high obliquity planets have higher annual global oxygen fluxes from sea to air than their low-obliquity equivalents (Figures 2(b), 3(b), 5(a)–(d)). Therefore, biospheres on moderately high obliquity exoplanets may be easier to detect than on their equivalent low-obliquity counterparts owing to their higher atmospheric oxygenation potential.

Oxygen is not the only potential biosignature that is enhanced by moderately high obliquity. Olson et al. (2018) explored the potential for the use of seasonality as a biosignature, in which the seasonal increase and decrease of biogenic gases such as CO_2, CH_4, O_2, and O_3 due to seasonal variation in insolation could be detectable by a LUVOIR-like instrument and indicate the presence of an active biosphere. As we have seen here on Earth, CO_2 and O_2 oscillate seasonally owing to changes in the balance of photosynthesis (draw down CO_2, make O_2) and respiration (release CO_2, consume O_2) (Keeling et al. 2001). While Earth has relatively moderate seasonality, exoplanets with higher obliquities would have more intense seasonality with large changes in temperature. As seasonal changes in the environment manifest as changes in atmospheric composition, larger seasonal differences may result in a larger, more detectable atmospheric signal (Olson et al. 2018).

4.3. Challenges for Life on Moderately High Obliquity Planets

While aquatic life is protected from seasonality owing to the high heat capacity of water, land environments may experience extreme seasonality on moderately high obliquity planets. This could be a problem because terrestrial microbes and ectothermic organisms are unable to regulate their own body temperatures (e.g., Hochachka & Somero 1977; Wright & Cooper 1981; Cossins & Bowler 1987; Huey & Kingsolver 1989) and therefore would be unlikely to survive the temperature extremes on land resulting from increased seasonality (similar to predictions by Paaijmans et al. 2013 of exotherm response to temperature variations caused by climate change on Earth). Additionally, while evolved terrestrial life that self-regulates body temperature (endotherms) can survive more extreme temperatures than ectotherms (e.g., Scholander et al. 1950; Irving & Krog 1954; Heinrich 1977; Lovegrove et al. 1991; McNab 2002), many adaptations to either extremely cold or hot environments are incompatible, such as fur or blubber.

Intensified seasonality does not have to be a death sentence for terrestrial life on moderately high obliquity planets, however. Multiple microbial species and a few multicellular species have been discovered living in extreme environments on Earth, including those at extremely cold and hot temperatures (e.g., Cavicchioli 2002). Life evolving on a planet with extreme seasons could potentially adapt to both extreme warm and cold climates and ultimately be more resilient against sudden environmental changes or mass extinctions.

Another potential problem for the origin and evolution of life on moderately high obliquity planets is water loss. Kang (2019b) found that high-obliquity planets have a much higher seasonal stratospheric water vapor abundance in comparison to equivalent low-obliquity planets, which may allow more water vapor to be lost owing to photodissociation and hydrodynamic escape of hydrogen to space. This potential for increased water loss suggests that liquid water on high-obliquity planet surfaces could be lost quickly, potentially endangering the origin/evolution of life on these planets, as liquid water is a key requirement for life. However, Kang (2019b) was looking at planets with obliquities higher than those considered in this work, so moderately high obliquity planet atmospheres may not experience the wetter stratospheres seen in higher-obliquity planet atmospheres. Additionally, potential water loss may be mitigated by the fact that wetter stratospheres only occurred seasonally in simulations from Kang (2019b) and may average out to negligible increased water loss on long-term average for high-obliquity exoplanets and their moderately high obliquity counterparts.

4.4. Opportunities for Future Work

Our results suggest that moderately high obliquity planets may experience both higher export POC production and higher oxygenation potential than their low-obliquity counterparts. However, as we only simulate planetary obliquities up to 45°, it is still unknown how the biospheres on higher-obliquity planets will fare under the physical and climatic changes that occur at higher obliquities. At planetary obliquities greater than 54°, the planet enters a different climate regime where the poles begin to receive more incident insolation than the equatorial regions, potentially leading to the formation of equatorial ice belts (e.g., Kilic et al. 2017, 2018; Rose et al. 2017; Colose et al. 2019). These equatorial ice belts would cause changes to both ocean circulation and surface wind fields, which may have significant effects on biospheric activity. We did not explore these obliquity scenarios because imposing annually averaged winds from ROCKE-3D would likely become an increasingly poor assumption at very high obliquities. Modeling biospheric dynamics and oxygenation potential on planets with higher obliquities remains an opportunity for future work.

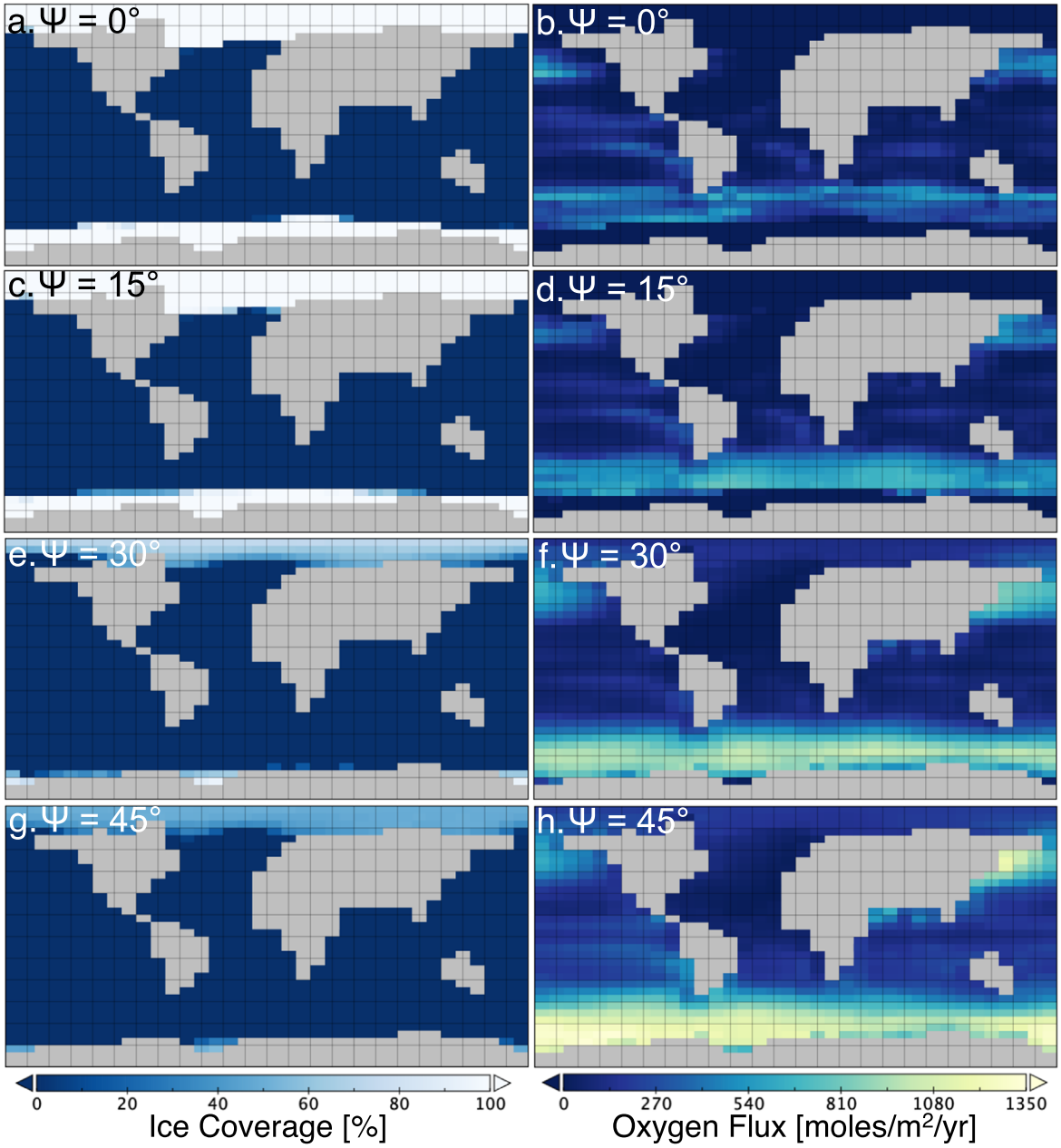

Figure 8. Global maps of annual average sea-ice cover percentage and oxygen flux for simulations with POL phosphate inventory and RLS. We consider obliquities of 0° (panels (a)/(b)), 15° (panels (c)/(d)), 30° (panels (e)/(f)), and 45° (panels (g)/(h)). The left color bar denotes the percentage of sea-ice cover in each area box, while the right color bar denotes annual average oxygen flux from each quadrant. The gray regions correspond to areas of land coverage, where ice coverage and oxygen flux are not measured.

5. Conclusions

We simulated Earth-like marine life on an Earth-sized planet at various obliquities. We found that moderately high obliquity promotes increased photosynthetic activity and associated oxygen flux to the atmosphere, potentially enhancing atmospheric oxygenation. Sea-to-air oxygen fluxes are further amplified by decreasing sea surface ice coverage at high latitudes on moderately high obliquity planets, exposing greater ocean surface area for sea-to-air gas exchange. This oxygenation may ultimately be beneficial for the evolution of complex life on moderately high obliquity planets (e.g., Catling et al. 2005; Reinhard et al. 2016). In short, our results suggest that life may not just survive but also thrive at moderately high obliquity.

Active biospheres may be easier to detect on moderately high obliquity planets as well. Increased planetary oxygenation on moderately high obliquity planets could result in easier detection of biogenic oxygen on moderately high obliquity planets with next-generation telescope concepts and potential earlier evolution of complex life (e.g., Catling et al. 2005; Reinhard et al. 2016). Additionally, life on moderately high obliquity planets may be easier to detect through heightened variations in biosignature gases over more intense seasonal cycles. Given the potential for increased biological activity and oxygenation on moderately high obliquity planets, the habitability and biosignatures of moderately high obliquity planets are exciting opportunities for future work.

ORCID iDs

Megan N. Barnett https://orcid.org/0000-0003-4804-577X
Stephanie L. Olson https://orcid.org/0000-0002-3249-6739

References

Armstrong, J., Barnes, R., Domagal-Goldman, S., et al. 2014, AsBio, 14, 277
Bills, B. G. 1990, JGR, 95, 14137
Bryan, M. L., Chiang, E., Bowler, B. P., et al. 2020, AJ, 159, 181
Catling, D. C., Glein, C. R., Zahnle, K. J., & McKay, C. P. 2005, AsBio, 5, 415
Cavicchioli, R. 2002, AsBio, 2, 281
Colose, C. M., Genio, A. D. D., & Way, M. J. 2019, ApJ, 884, 138
Cossins, A. R., & Bowler, K. 1987, Temperature Biology of Animals (Dordrecht: Springer)
Guendelman, I., & Kaspi, Y. 2019, ApJ, 881, 67
Heinrich, B. 1977, The American Naturalist, 111, 623
Hochachka, P. W., & Somero, G. N. 2016, Biochemical Adaptation (Princeton, NJ: Princeton Legacy Library), https://press.princeton.edu/books/hardcover/9780691640556/biochemical-adaptation
Huey, R. B., & Kingsolver, J. G. 1989, Trends in Ecology & Evolution, 4, 131
Irving, L., & Krog, J. 1954, JAPh, 6, 667
Kang, W. 2019a, ApJL, 876, L1
Kang, W. 2019b, ApJL, 877, L6
Keeling, C. D., Piper, S. C., Bacastow, R. B., et al. 2001, in A History of Atmospheric CO2 and Its Effects on Plants, Animals, and Ecosystems. Ecological Studies, ed. I. T. Baldwin et al. (New York: Springer)
Kilic, C., Lunkeit, F., Raible, C. C., & Stocker, T. F. 2018, ApJ, 864, 106
Kilic, C., Raible, C. C., & Stocker, T. F. 2017, ApJ, 844, 147
Komacek, T. D., Kang, W., Lustig-Yaeger, J., & Olson, S. L. 2021, Eleme, 17, 251
Laskar, J., Correia, A. C. M., Gastineau, M., et al. 2004, Icar, 170, 343
Laskar, J., & Robutel, P. 1993, Natur, 361, 608
Linsenmeier, M., Pascale, S., & Lucarini, V. 2015, P&SS, 105, 43
Lovegrove, B. G., Heldmaier, G., & Ruf, T. 1991, Journal of Thermal Biology, 16, 185
Lustig-Yaeger, J., Meadows, V. S., & Lincowski, A. P. 2019, AJ, 158, 27
Lyons, T. W., Reinhard, C. T., & Planavsky, N. J. 2014, Natur, 506, 307
McNab, B. K. 2002, The Physiological Ecology of Vertebrates: A View from Energetics (Ithaca, NY: Cornell Univ. Press)
Meadows, V. S., Reinhard, C. T., Arney, G. N., et al. 2018, AsBio, 18, 630
Nowajewski, P., Rojas, M., Rojo, P., & Kimeswenger, S. 2018, Icar, 305, 84
Olson, S. L., Jansen, M., & Abbot, D. S. 2020, ApJ, 895, 19
Olson, S. L., Kump, L. R., & Kasting, J. F. 2013, ChGeo, 362, 35
Olson, S. L., Reinhard, C. T., & Lyons, T. W. 2016, PNAS, 113, 11447
Olson, S. L., Schwieterman, E. W., Reinhard, C. T., et al. 2018, ApJL, 858, L14
Paaijmans, K. P., Heinig, R. L., Seliga, R. A., et al. 2013, GCBio, 19, 2373
Palubski, I. Z., Shields, A. L., & Deitrick, R. 2020, ApJ, 890, 30
Planavsky, N. J., Asael, D., Hofmann, A., et al. 2014, NatGe, 7, 283
Reinhard, C. T., Olson, S. L., Kirtland Turner, S., et al. 2020, GMD, 13, 5687
Reinhard, C. T., Planavsky, N. J., Gill, B. C., et al. 2017, Natur, 541, 386
Reinhard, C. T., Planavsky, N. J., Olson, S. L., Lyons, T. W., & Erwin, D. H. 2016, PNAS, 113, 8933
Ridgwell, A., Hargreaves, J. C., Edwards, N. R., et al. 2007, BGeo, 4, 87
Rose, B. E. J., Cronin, T. W., & Bitz, C. M. 2017, ApJ, 846, 28
Scholander, P. F., Hock, R., Walters, V., & Irving, L. 1950, The Biological Bulletin, 99, 259
Spiegel, D. S., Menou, K., & Scharf, C. A. 2009, ApJ, 691, 596
Tyrrell, T. 1999, Natur, 400, 525
Wang, J., Mawet, D., Hu, R., et al. 2018, JATIS, 4, 035001
Wang, Y., Liu, Y., Tian, F., et al. 2016, ApJL, 823, L20
Wanninkhof, R. 2014, LimOc, 12, 351
Way, M. J., Aleinov, I., Amundsen, D. S., et al. 2017, ApJS, 231, 12
Williams, D. M., & Kasting, J. F. 1997, Icar, 129, 254
Williams, G. E. 1993, ESRv, 34, 1
Wright, R. K., & Cooper, E. L. 1981, Developmental & Comparative Immunology, 5, 117